Applied Thermal Engineering 211 (2022) 118384

Contents lists available at ScienceDirect

Applied Thermal Engineering

journal homepage: www.elsevier.com/locate/ate

Research paper

Preliminary investigation on the adoption of CO_2-SO_2 working mixtures in a transcritical Recompression cycle

Francesco Crespi *, Pablo Rodríguez de Arriba, David Sánchez, Antonio Muñoz

Department of Energy Engineering, University of Seville, Camino de los descubrimientos s/n, 41092 Seville, Spain

ARTICLE INFO

Keywords:
Supercritical Carbon Dioxide
Power cycle
Mixture
Thermodynamic
Recompression
Sulphur Dioxide

ABSTRACT

This paper investigates the interest and potential of using working fluids based on Carbon and Sulphur Dioxide mixtures (CO_2-SO_2) in a transcritical *Recompression* cycle. In order to assess the actual thermodynamic potential of the concept proposed, the influence of dopant (SO_2) content is assessed for two different turbine inlet temperatures (550 °C and 700 °C). The results obtained are compared with other CO_2 mixtures already proposed in literature (CO_2-C_6F_6 and CO_2-$TiCl_4$)) and for two alternative cycle layouts (*Recuperated Rankine* and *Precompression*).

The results pf the analysis reveal that, at high ambient temperature, the *Recompression* cycle operating on CO_2-SO_2, with Sulphur Dioxide content between 20% and 30%(v), is a very interesting option for Concentrated Solar Power plants, able to achieve thermal efficiencies ≈45% and >51% at 550 °C and 700 °C respectively. At a minimum cycle temperature of 50 °C, the proposed configuration leads to thermal efficiency gains of 6% and 2% with respect to the *Brayton* and *Recompression* cycles working on pure CO_2. This performance enhancement of the *Recompression* cycle with CO_2-SO_2 is comparable to or higher than that enabled by other CO_2 mixtures proposed in literature, but with significantly higher specific work (smaller footprint) and temperature rise across the solar receiver (lower installation costs).

1. Introduction

The scientific community and industry agree on the potential of Supercritical Carbon Dioxide (sCO_2) cycles for next generation CSP plants, owing to their high thermal efficiency and arguably smaller footprint. The growing interest in this technology can be monitored through the large number of publications on the topic produced in the last fifteen years. These have discussed aspects of the technology such as thermodynamic assessment of cycles [1,2], aerothermal and mechanical design of components [3–5], system integration [6–8] and economic analysis [9,10]. Nevertheless, the technology is also acknowledged to have a critical weakness stemming from the need to carry out compression near the critical point of CO_2 (31.04 °C, 73.88 bar), in order to unleash the thermodynamic potential of these cycles. When this is not the possible, for instance due to high ambient temperatures (usual in CSP applications), compressor inlet temperature increases and the thermal performance of sCO_2 power systems drops dramatically. This is inherent to the properties of Carbon Dioxide and cannot be compensated for by the adoption of advanced layouts which, in addition to not solving the problem, are very likely to increase installation costs prohibitively [11].

In order to solve this problem, several authors have investigated the utilisation of working fluids based on CO_2 mixtures where certain chemical compounds are added to the raw CO_2 flowing in the system: Invernizzi and Van der Stelt [12], and recently Siddiqui [13], explore the potential of mixtures based on CO_2 and hydrocarbons; Baik and Lee provide a preliminary analysis of the potential of CO_2–R32 mixtures using experimental data [14]; and Manzolini et al. [15] present a techno-economic assessment of cycles using this concept in Concentrated Solar Power applications.

The SCARABEUS project, funded by the Horizon 2020 programme of the European Commission [16], follows this pathway. In this project, the addition of certain dopants to Carbon Dioxide yields a mixture with higher critical temperature than pure CO_2, enabling compression of the working fluid close to its critical temperature even in hot environments ($T_{a,b}$ ≈ 50 °C) [17,18]. The concept will be demonstrated experimentally at a dedicated rig during the project.

Previous works by the authors of this paper, within the context of the SCARABEUS project, investigated the thermal performance gains enabled by mixtures of Carbon Dioxide and Titanium Tetrachloride

* Corresponding author.
E-mail addresses: crespi@us.es (F. Crespi), prdearriba@us.es (P. Rodríguez de Arriba), ds@us.es (D. Sánchez), ambl@us.es (A. Muñoz).

https://doi.org/10.1016/j.applthermaleng.2022.118384
Received 27 September 2021; Received in revised form 18 March 2022; Accepted 20 March 2022
Available online 27 March 2022

Nomenclature

α	Split Flow Factor [–]
ΔP_{HX}	HX Pressure drop [%]
ΔT_{gap}	Difference between T_{cr} and T_{min} [°C]
ΔT_{PHE}	Temperature rise across PHE [%]
ΔT_{pp}	Minimum temperature difference in HX (pinch point) [°C]
$\dot{m}$	Mass flow [kg/s]
η_{is}	Isentropic Efficiency [%]
η_{th}	Cycle Thermal Efficiency [%]
ρ	Specific Mass [kg/m^3]
CSP	Concentrated Solar Power
h	Enthalpy [J/kg]
$HTRec$	High Temperature Recuperator
LCA	Life Cycle Assessment
$LTRec$	Low Temperature Recuperator
MW	Molar Weight [kg/kmol]
P_{cr}	Critical Pressure [bar]
P_{max}	Maximum Cycle Pressure [bar]
PHE	Primary Heat Exchanger
PIT	Pump Inlet Temperature [°C]
pp	Percentage point [%]
s	Entropy [J/kgK]
sCO_2	Supercritical Carbon Dioxide
T_{cr}	Critical Temperature [°C]
T_{min}	Cycle minimum temperature [°C]
TIT	Turbine Inlet Temperature [°C]
$W_{s,VOL}$	Specific Work-volumetric base [MJ/m^3]
W_s	Specific Work [kJ/kg]
y	Molar fraction of dopant [–]
Z	Compressibility Factor [–]

($TiCl_4$) or Hexafluorebenzene (C_6F_6) in power cycles [18–20]. A thorough literature review of supercritical cycles, with emphasis on transcritical condensing cycles, showed that the *Recuperated Rankine* and *Precompression* layouts were able to fully exploit the potential of CO_2–$TiCl_4$ and CO_2–C_6F_6 mixtures respectively. These results are expanded to mixtures of CO_2 and Sulphur Dioxide (SO_2) in this paper, with the aim to identify (i) the potential for performance enhancement enabled by this dopant, and (ii) the cycle layout yielding larger performance gains. As shown later in the paper, it is observed that the *Recompression* cycle achieves very good performance with this mixture and, therefore, it is added to the *Recuperated Rankine* and *Precompression* layouts for a detailed analysis.

This is the first time a transcritical *Recompression* cycle using CO_2–SO_2 mixtures is presented in literature, to the authors' best knowledge, although partly related works must be acknowledged. Tafur-Escanta et al. investigated four different CO_2-based mixtures, including 90%CO_2–10%SO_2 in a supercritical *Recompression* power cycle coupled to a solar thermal parabolic-trough plant, concluding that CO_2–SO_2 mixtures could improve cycle efficiency by 3% [21]. Wang et al. presented a similar approach, considering different dopants in either *Recuperated Brayton* or *Recompression* cycles, and found that adding 5% SO_2 in a *Recompression* cycle could increase thermal efficiency by about 2% with respect to the same layout with pure CO_2 [22]. Rath et al. also considered SO_2 in a wide analysis of the *Simple Recuperated* cycle operating on CO_2 mixtures with 135 different dopants [23]. The authors found that only marginal gains in terms of thermal efficiency (<1%) were possible with respect to the same cycle using pure CO_2. Finally, another paper developed in the framework of the SCARABEUS project and authored by Aqel et al. has recently looked into the impact that using CO_2 mixtures with SO_2, $TiCl_4$ and C_6F_6 has on turbine design for a *Recuperated Rankine* cycle [24].

Based on this past work by the same and other authors, the paper is organised as follows. In the first part of the paper, a brief characterisation of Sulphur Dioxide is provided, along with a discussion regarding the main features of CO_2–SO_2 mixtures. Then, the thermal performances enabled by transcritical *Recompression* cycles operating on this non-conventional fluid are assessed, considering two different turbine inlet temperatures (550 °C and 700 °C) and comparing the results with other layouts (*Recuperated Rankine* and *Precompression*) and dopants (C_6F_6, $TiCl_4$). Finally, a comparison of the foregoing cases against a *Recompression* cycle using pure CO_2 is presented in order to investigate the actual applicability and potential of the concept proposed in the paper.

2. Characterisation of Sulphur Dioxide and definition of candidate mixtures

Sulphur Dioxide is a colourless gas widely employed in the industry for applications such as food preservation (antiseptic) or refrigeration [25,26]. Characterised by a pungent odour, SO_2 is produced both naturally (volcanic eruptions) or via anthropogenic activity, primarily combustion of fossil fuels (coal and oil) and smelting of minerals containing sulphur (copper, lead) [27]. It presents high solubility in several organic solvents, extremely high thermal stability and it is neither explosive nor flammable [28]. On the other hand, the compound is highly irritant and classifies as Level 3 for health hazard according to NFPA-704 standards [29] and safety group B1 by ASHRAE [30]. When inhaled, usual symptoms range from nasal inflammation to bronchoconstriction but there is limited evidence of chronic toxicity, generally similar to chronic bronchitis without the involvement of bacterial infection [31].

The characteristics of the dopants considered in the SCARABEUS project are presented in Table 1, based on the NFPA-704 standard. Other refrigerants and thermal oils are also listed in the Table for the sake of comparison. It is observed that Sulphur Dioxide exhibits less safety-related issues and better reliability than other dopants considered in earlier phases of the project: Hexafluorobenzene (C_6F_6, high flammability) or Titanium Tetrachloride ($TiCl_4$, high water reactivity). The health hazard characteristics of SO_2 are similar to those of Therminol VP-1 (widely employed in Concentrated Solar Power plants using parabolic-trough technology), and significantly safer than Ammonia, a very common refrigerant classified as B2L according to ASHRAE. Similarly, other state-of-the-art refrigerants such as propane (R-290) or R-1234yf, common in air-conditioning and refrigeration systems, exhibit values comparable to those of SO_2 in the NFPA-704 classification system.

It is worth noting that the characteristics of Sulphur Dioxide are not far from those of CO_2, which is a simple asphyxiant gas classifying as Level 2 for health hazard, and these similarities extend to the thermodynamic features of the compounds. In particular, Table 2 shows that both SO_2 and CO_2 present very high thermal stability — significantly higher than C_6F_6 or $TiCl_4$ — and very similar critical pressure and molecular complexity.[1] A concern about using CO_2–SO_2 mixtures in supercritical power cycles is the risk to experience corrosion promoted by SO_2 on wet metal surfaces [34,35], as a consequence of the creation of sulphuric acid (H_2SO_4) when SO_2 reacts with water. This is currently under investigation in oxycombustion applications which naturally contain traces of SO_2 and a substantial amount of H_2O as a consequence of combustion (for instance, the *Allam* cycle [36]). In Concentrated Solar Power applications operating on CO_2–SO_2 mixtures,

[1] The molecular complexity has been estimated as $(T_c/R)\cdot(dS/dT)_{T_R=0.7}$, see page 109 in Ref. [32].

Table 1
Hazards of different fluids according to NFPA 704 [29].

	Health hazard	Flammability	Chemical reactivity	Special hazard
CO_2	2	0	0	Simple Asphyxiant
SO_2	3	0	0	–
C_6F_6	1	3	0	–
$TiCl_4$	3	0	2	Reacts with water
Ammonia	3	3	0	–
R-290	2	4	0	–
R-1234yf	1	4	0	–
Therminol 66	1	1	0	–
Therminol VP-1	2	1	0	–

Table 2
Thermodynamic properties of Carbon Dioxide and the three dopants considered in the SCARABEUS project.

	MW [kg/kmol]	T_{cr} [°C]	P_{cr} [bar]	Molecular complexity [–]	Thermal Stability
CO_2	44.01	31.06	73.83	−9.324	>700 °C [28]
SO_2	64.06	157.60	78.84	−8.230	>700 °C [28]
C_6F_6	186.06	243.58	32.73	12.740	up to 625 °C[a]
$TiCl_4$	189.69	364.85	46.61	1.922	up to 700 °C [33]

[a]Threshold temperature obtained by University of Brescia and Politecnico di Milano for the SCARABEUS project. Complete set of experimental results to be disclosed in a future publication by these two institutions.

there is no water formation because there is no combustion. This mitigates this risk to experience corrosion.

It is worth noting that the corrosion problem presented in the foregoing is different from that experienced in pure CO_2 applications, which is caused by material oxidation and observed even with advanced alloys [37–39]. This latter phenomenon is nevertheless applicable to either pure CO_2 or CO_2 mixtures and does not constitute a problem specific to supercritical power systems operating on sCO_2 mixtures. Moreover, the onset and severity of corrosion is a complex problem that falls out of the scope of the paper; hence, it is not discussed here.

The thermophysical properties of CO_2–SO_2 mixtures are calculated with Aspen Properties v11.0, using a standard Peng–Robinson Equation of State (PR EoS), calibrated on experimental data of the corresponding Vapour–Liquid-Equilibrium (VLE) conditions [40]. This dataset is provided by University of Brescia and Politecnico di Milano, partners of the SCARABEUS consortium, who also worked on identifying SO_2 as a potential dopant. It is to note that the behaviour of the mixture has been estimated with other models, in addition to the standard PR EoS: copolymer PC-Saft model (PC-SAFT), Lee-Kleser Plocker (LK-Plock) and Nist-REFPROP method. The results of this assessment, to be disclosed soon in publication by the aforementioned institutions, reveal that using PR and PC-Saft yields the best match to the experimental and literature data available, even if with slight differences: PR yields a better estimate of the critical pressure and temperature of the mixture whilst PC-Saft seems to be the best option for an overall assessment of the thermophysical properties of the mixtures, in particular when speed of sound and residual heat capacity are relevant. These parameters are of utmost importance for the thermo-mechanical design of cycle components, especially turbomachinery, but their effect on the preliminary assessment of cycle performance is very weak. More information about this latter influence is provided in Appendix of the present manuscript, where using different EoS is proved to bring about thermal efficiency variations lower than 1.5% (≈0.6 percentage points in absolute terms), regardless of the dopant content and operating temperatures of the cycle. Therefore, for the sake of simplicity and consistence with previous works by the authors, the standard PR Equation of State is used in the present manuscript.

In previous studies by the authors of this paper [18], the minimum molar fraction of dopant was set to yield a critical temperature of the mixture of ≈80 °C. This value provides a 30 °C gap between the minimum cycle temperature (T_{min}, set to 50 °C for the reference case in a hot environment) and the critical temperature of the working fluid (T_{cr}), thus enabling condensation even in the most adverse conditions (i.e., highest ambient temperature). This yields minimum molar fractions of 10% and 14% when using C_6F_6 and $TiCl_4$ respectively, values that are lower than the optimum dopant content for peak thermal efficiency (see Table 3). For Sulphur Dioxide, the same constraint corresponds to a minimum molar fraction of 30%SO_2, significantly higher than for the other compounds. This is due to the substantially lower critical temperature of SO_2, see Table 2, affecting the Pressure–Temperature (p-T) envelopes and the critical loci of the mixtures. A graphical description of this is provided in Fig. 1(a), where a 70%CO_2–30%SO_2 mixture is compared to 85%CO_2–15%C_6F_6 and 85%CO_2–15%$TiCl_4$, the two mixtures yielding the best cycle performance with Hexafluorobenzene and Titanium Tetrachloride respectively [18]. The case for pure CO_2 is also shown for comparison. The effect of composition on the shape of p-T envelopes for the three dopants is visible, both in terms of position of the critical point and width of the envelope. This last aspect, also called temperature glide (dashed lines in Fig. 1(a)), is proportional to the difference between the critical temperature of Carbon Dioxide and the critical temperature of the dopant, and it is crucial for the feasibility of some supercritical CO_2 cycles operating on mixtures (this is explained further in the last section of the paper).

Further to the foregoing discussion, Carbon Dioxide mixtures with Sulphur Dioxide have a very relevant difference with both CO_2–C_6F_6 and CO_2–$TiCl_4$. For the latter two mixtures, the dopant fractions (of C_6F_6 and $TiCl_4$) yielding peak cycle efficiency have critical temperatures higher than 80 °C. This is however not the case for SO_2, whose optimum SO_2 fraction efficiency-wise is lower than 30% (it is reminded here that a 70/30 CO_2–SO_2f mixture has a critical temperature of ≈80 °C). This means that the 30 °C temperature gap (ΔT_{gap}) between minimum cycle temperature and critical temperature of the mixture is actually constraining the design space of the cycle in the quest for higher efficiencies. In the light of this, and in order to explore potential efficiency gains beyond this constraint, it is decided to reduce the minimum molar fraction of SO_2 allowed to 20%, which corresponds to a ΔT_{gap} of about 15 °C. The characteristics of three representative mixtures with 20, 30 and 40%(v) SO_2 content are summarised in Table 3 along with those of the optimum mixtures with $TiCl_4$ and C_6F_6 (peak cycle efficiency). As usual, the following standard code is used to label each mixture: DxCyy, where x identifies the dopant (1 = C_6F_6, 2 = $TiCl_4$, 3 = SO_2) and yy represent the corresponding molar fraction.

3. Computational environment and cycle modelling

The system has been modelled with Thermoflex v.29, a commercial software developed by Thermoflow Inc. [41], with the thermophysical properties of the working mixtures incorporated in the form of look-up tables. These look-up tables have been produced with Aspen

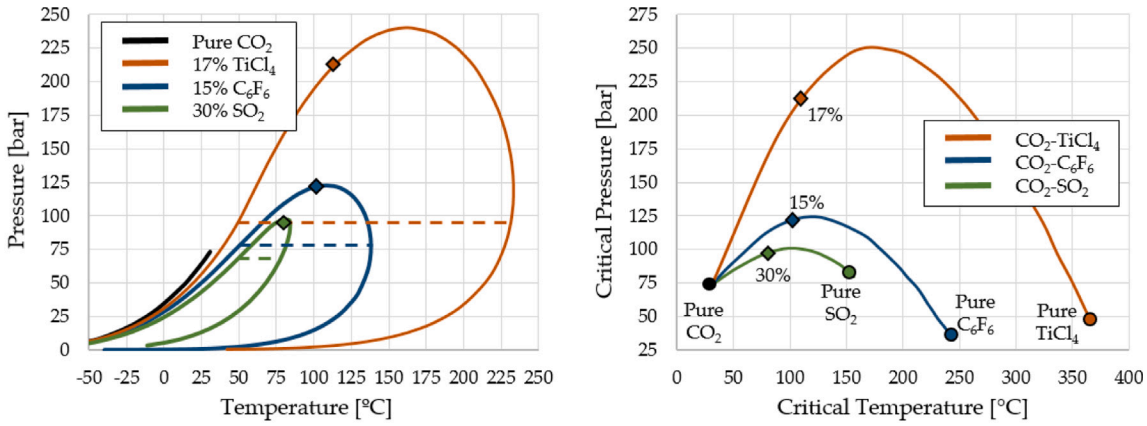

(a) Pressure-Temperature envelopes for different SCARABEUS mixtures.

(b) Critical Loci of the three dopants considered.

Fig. 1. Pressure–Temperature envelopes for three different mixtures and pure CO_2 (left) and critical loci for the three dopants (right). In Figure (a), critical points are represented by markers while temperature glides for a bubble temperature of 50 °C are indicated with dotted lines.

Table 3
Main characteristics of working fluids. P_{cond} and temperature glide refer to a bubble temperature of 50 °C.

Mixture	Molar comp. [%]	MW [kg/kmol]	T_{cr} [°C]	P_{cr} [bar]	P_{cond} [bar]	Glide [°C]
D1C15	CO_2–C_6F_6 [85–15]	65.32	102.1	121.3	77.52	88.4
D2C17	CO_2–$TiCl_4$ [83–17]	68.77	116.4	212.6	96.17	181.6
D3C20	CO_2–SO_2 [80–20]	48.03	64.2	91.85	77.41	16.1
D3C30	CO_2–SO_2 [70–30]	50.03	79.47	97.51	68.53	27.99
D3C40	CO_2–SO_2 [60–40]	52.03	93.79	100.5	60.12	38.55

Table 4
Boundary conditions and specifications of turbomachinery and heat exchangers.

PIT [°C]	TIT [°C]	P_{max} [bar]	η_{is} [%] Pump/Turb/Compr	ΔT_{min} [°C]	ΔP_{heater} [bar]	ΔP_{cond} [bar]	ΔP_{rec} [%] Low P/High P
50	550/700	250	88/93/89	5	1.5	0	1/1.5

by University of Brescia and Politecnico di Milano [42] and then added to Thermoflex through *User-defined fluid* tool specifically developed by Thermoflow for the SCARABEUS project. At this preliminary stage, the main cycle components (heat exchangers and turbomachinery) are modelled with lumped-volume models already built into the software.

The specifications of the reference power block are summarised in Table 4. Gross power output is set to 100 MW whilst two different turbine inlet temperatures are considered: 550 °C, corresponding to state-of-the-art tower-type CSP plants, and 700 °C, representative of next-generation receiver technology. The effects of varying minimum cycle temperature, isentropic efficiency of turbomachinery and minimum temperature difference of recuperators are investigated as well, considering values in the following ranges respectively: 30 °C–60 °C, 80%–100% and 5–25 °C.

Three cycle layouts are considered, whose schematic representations are shown in Fig. 2: *Recuperated Rankine*, *Precompression* and *Recompression* [43]. The two first layouts, *Recuperated Rankine* and *Precompression*, are the most interesting options for CO_2–$TiCl_4$ and CO_2–C_6F_6 mixtures as credited in previous works by the authors [18]. On the other hand, the *Recompression* cycle is very likely the most well-known sCO_2 cycle and has been investigated widely in literature. Here, the cycle is adopted in a transcritical embodiment, in order to exploit the potential of CO_2–SO_2 mixtures in condensing cycles.

4. Discussion of results

4.1. Best-performing mixture and layout

The thermal performance of the three cycles considered, as a function of the molar content of SO_2, is presented in Fig. 3. Thermal efficiency (η_{th}) and specific work (W_s) are the main figures of merit while the inlet temperature to the Primary Heat Exchanger (PHE) and turbine outlet pressure are complementary parameters of interest. As indicated in the legend, the blue, orange and green lines correspond to the *Recuperated Rankine*, *Precompression* and *Recompression* cycles respectively. For all these cases, dashed lines apply to a turbine inlet temperature of 550 °C and solid lines to 700 °C.

A first observation in Fig. 3(a) is the monotonically decreasing trend of thermal efficiency for increasing SO_2 concentration, with a slope that depends weakly on cycle configuration and is similar for both turbine inlet temperatures considered. In a closer look, the *Precompression* cycle at 700 °C presents the largest slope, changing from 47.1% for 20% SO_2 (D3C20) to 45.7% for 40% SO_2 (D3C40), whilst the thermal efficiency of the *Recuperated Rankine* cycle operating at 550 °C remains approximately constant regardless of the molar fraction of SO_2 (thermal efficiency varies by 0.4 percentage points in the range under analysis). Specific work presents the opposite trend, increasing in parallel with the molar fraction of Sulphur Dioxide, Fig. 3(b). Relative variations of this figure of merit range from 8.6% (*Recompression* cycle at 700 °C) to 13% (*Recuperated Rankine* cycle at 700 °C).

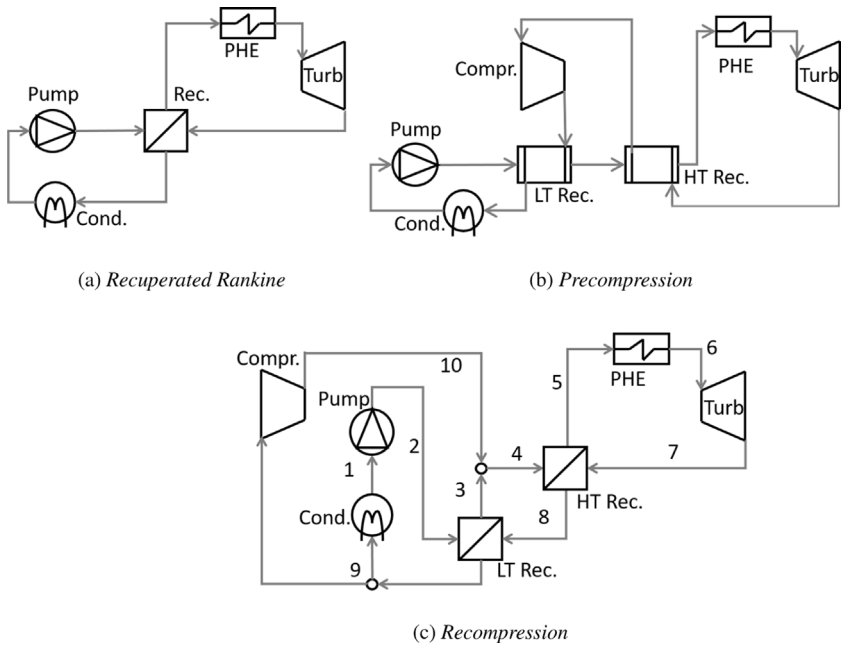

(a) *Recuperated Rankine* (b) *Precompression*

(c) *Recompression*

Fig. 2. Cycle layouts considered in the analysis.

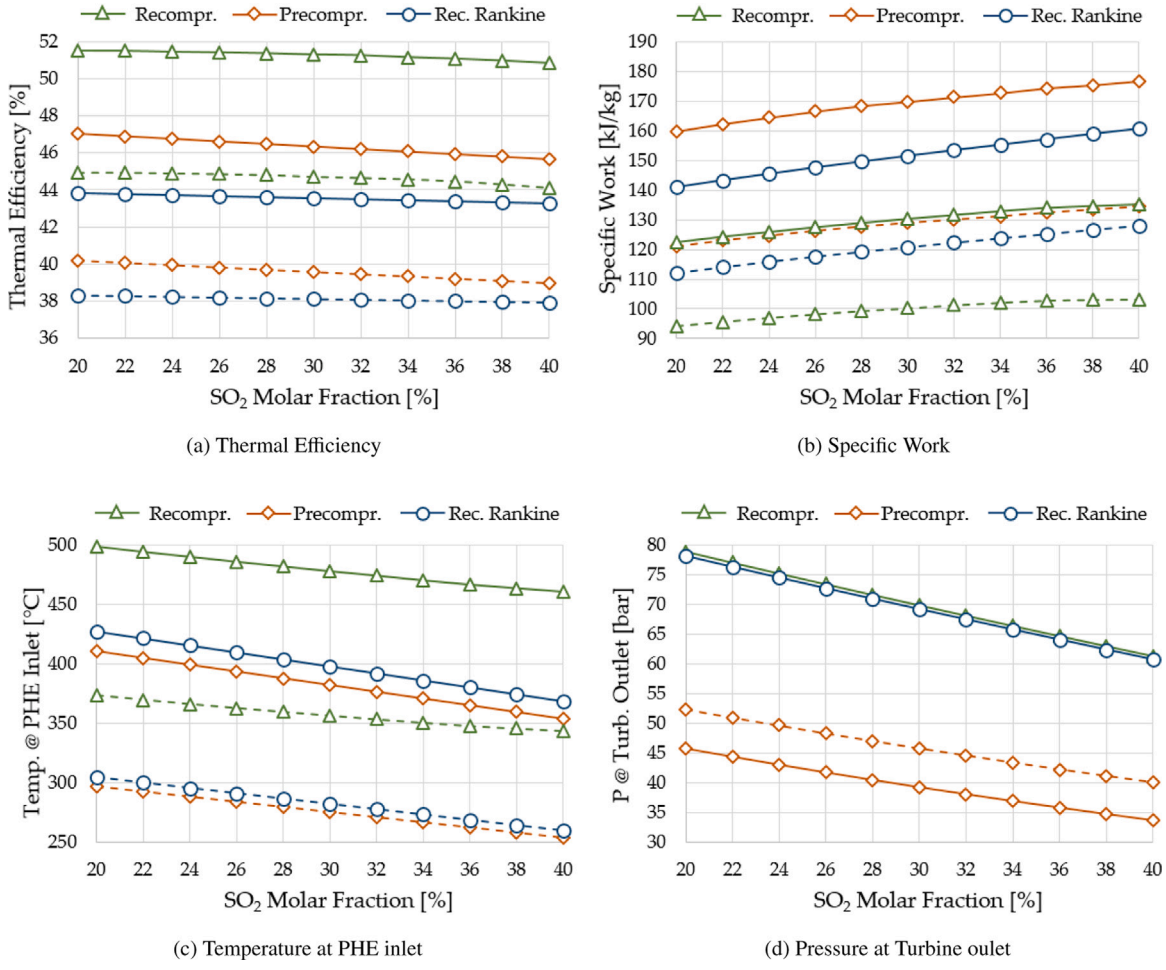

(a) Thermal Efficiency (b) Specific Work

(c) Temperature at PHE inlet (d) Pressure at Turbine oulet

Fig. 3. Influence of SO_2 content on the performance of transcritical cycles working on CO_2 mixtures. Dashed lines correspond to TIT = 500 °C. Solid lines correspond to 700 °C.

Fig. 3 also confirms that the *Recompression* cycle is very interesting when CO_2–SO_2 mixtures are used. For a turbine inlet temperature of 550 °C, this configuration yields $\eta_{th} \approx 45\%$, whilst the *Recuperated Rankine* and *Precompression* layouts hardly achieve 38.5% and 40.5%

respectively. Moreover, this superior performance of the *Recompression* cycle is so clear that it achieves similar efficiency at 550 °C than the other cycle layouts at 700 °C. This puts the *Recompression* cycle operating at 550 °C forward as a very interesting alternative for CSP applications, achieving thermal efficiencies higher than subcritical or even supercritical steam turbines using state-of-the-art receiver technology (≈42%, for a minimum cycle temperature of 50 °C [18]). At 700 °C, the *Recompression* cycle on a 70%CO_2/30%SO_2 mixture outperforms both *Precompression Recuperated Rankine* by a margin larger than 5 percentage points efficiency wise.

In a closer look, the key feature of the *Recompression* cycle to enable higher efficiencies is a significant reduction of exergy losses in the recuperator, as highlighted by Angelino originally [43]. This is thanks to the balanced heat capacities on both sides of this heat exchanger, brought about by the lower mass flow rate on the low pressure side of it (with higher specific heat at constant pressure c_p). In order to achieve this balance, the compression process is split in two parallel streams which experience compression with the same pressure ratio but different inlet temperatures and flow rates, Fig. 2(c). The outcome is a higher temperature at the inlet to the primary heat exchanger, Fig. 3(c), which translates into a higher thermal efficiency of the cycle.

On the negative side, compression work increases in a *Recompression* layout, inasmuch as part of the compression process takes place in gaseous state, thereby reducing the specific work W_s of the cycle. Compensating for this is actually the main driver of the *Precompression* cycle as explained by the results in Figs. 3(c–d) and 2. With respect to a reference *Recuperated Rankine* layout, the *Precompression* layout enables a significant reduction in turbine outlet pressure[2] and this brings about a parallel increase of specific work and thermal efficiency. This is so because the additional work of the precompressor installed in between the recuperators, see Fig. 2(b), is lower than the additional expansion work obtained from the turbine [43]. The gain in specific work does however not translate into a similar efficiency gain due to the lower turbine outlet temperature that limits the potential for internal heat recovery at the high temperature recuperator, Fig. 3(c). Yet, the slightly higher heat supply to the cycle is more than compensated for by the higher specific work, what has a positive impact on thermal efficiency overall.

The results shown in this section confirm that, regardless of cycle layout and turbine inlet temperature: (1) the minimum molar fraction of dopant (in the range studied) always yields maximum thermal efficiency; and (2) the highest specific work is obtained for the highest concentration of SO_2. A lower SO_2 content also leads to higher temperatures at the inlet to the primary heat exchanger (Fig. 3b, c) and, therefore, lower temperature rise across this component (ΔT_{PHE}). This has a direct impact on the temperature rise available in the solar receiver (i.e., operating temperature range of molten salts) and, therefore, on the size and cost of the Thermal Energy Storage system and of the entire Concentrated Solar Power plant [11]. Unfortunately, the compromise between these three figures of merit in a practical application (i.e., the composition of the optimum mixture) cannot be unequivocally identified without an overall techno-economic assessment based on capital cost and Levelised Cost of Energy, in addition to other considerations discussed in Section 2. For instance, a lower content of SO_2 is interesting from social and environmental standpoints, due to safety concerns regarding SO_2 leaking out from the system (highly irritant fluid), and it could also help reduce the higher maintenance costs that could be caused by corrosion. But at the same time, a lower SO_2 content would lead to a lower critical temperature of the mixture, thus a more challenging design and operation of the compression device (pump).

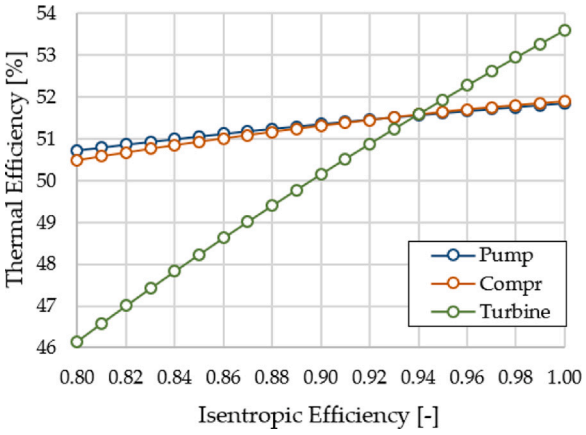

Fig. 4. Sensitivity of cycle efficiency to isentropic efficiency of turbomachinery. Results apply to a *Recompression* cycle working on 70%CO_2–30%SO_2 and 700 °C turbine inlet temperature.

Unfortunately, such a complex analysis cannot be carried out at present, given the early stage of development of some of the key components in the plant (not only major components but also Balance of Plant equipment), the lack of suitable cost-estimation tools and data to properly address the socio-environmental impact of this technology by means of LCA analysis.[3] This is why thermal efficiency is selected as the primary driver in this paper and why the optimum molar content of Sulphur Dioxide depends directly on the assumption made about the difference between T_{cr} and T_{min}, regardless of cycle layout and turbine inlet temperature. Using this approach, a 30% SO_2 content is selected for the conservative case of $\Delta T_{gap} = 30$ °C, whilst this content is reduced to 20% SO_2 if $\Delta T_{gap} = 15$ °C. For the sake of simplicity, and due to the very similar thermal performances presented by these two mixtures, the authors have decided to consider only the more conservative case in Sections 4.2, 4.3 and 5.

4.2. Influence of the performance of turbomachinery and recuperators

In this section, the effect of component efficiency on cycle performance is investigated for a *Recompression* cycle working on 70%CO_2–30%SO_2 and 700 °C turbine inlet temperature. The isentropic efficiency of each turbomachine (pump, compressor and turbine) is varied, one at a time, from 80% to 100% in 1% incremental steps and the resulting impact on cycle performance is shown in Fig. 4. As expected, turbine efficiency has the strongest impact on cycle efficiency, leading to a 10% η_{th} drop when changing from 93% to 80%. Despite this, 50% thermal efficiency can still be attained for turbine efficiencies ≥90%, a specification that is not uncommon in literature [5]. Furthermore, it is worth noting that thermal efficiency is always higher than 50% for any value of pump and compressor efficiency in the aforecited range.

The effect of recuperator performance is presented in Fig. 5. This plot reports the maximum thermal efficiency attainable and the corresponding split flow factor of a *Recompression* cycle when the pinch points of the recuperators take values between 5 and 25 °C. Results are provided for the individual and joint variation of pinch points in the high and low temperature recuperators, confirming that the influence of the low temperature recuperator is dominant (LT Rec in Fig. 2). A 20 °C rise in $\Delta T_{pp,LT\,Rec}$ leads to $\Delta\eta_{th} > 5\%$ whereas the same variation in $\Delta T_{pp,HT\,Rec}$ yields $\Delta\eta_{th} \approx 1.7\%$.

Another interesting feature in Fig. 5 is the symmetrical trend of the optimum split flow factor (α), defined as the fraction of fluid

[2] This parameter is representative of the minimum cycle pressure, which is now allowed to vary in order to maximise thermal efficiency [18].

[3] All these tasks are currently under development by the SCARABEUS consortium.

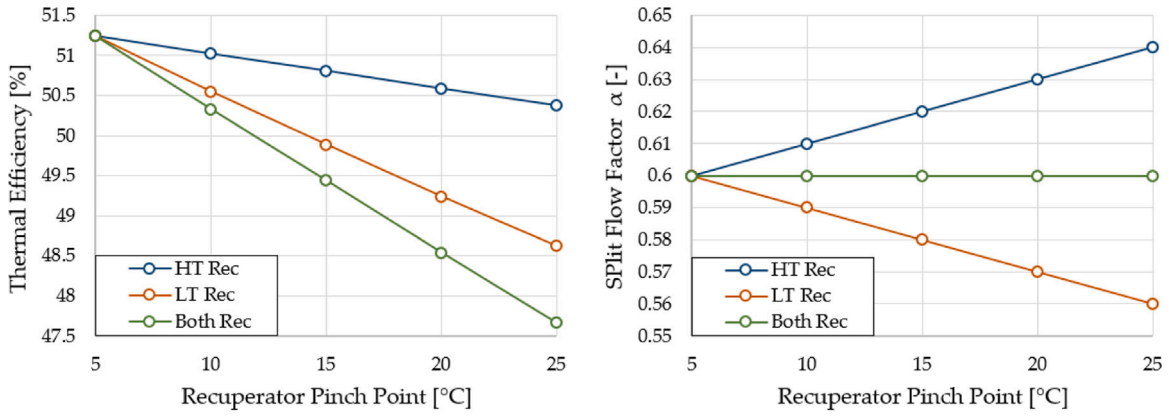

(a) Thermal Efficiency (b) Optimum Flow-Split Factor

Fig. 5. Sensitivity of cycle efficiency to recuperator pinch point (a), along with the corresponding values of split flow factor (b). Results apply to a *Recompression* cycle working on 70%CO_2–30%SO_2 and 700 °C.

flowing across the Low-Temperature Recuperator (stations 1-2-3 in Fig. 2(c)). In order to maximise thermal efficiency, α decreases when the performance of LT Rec deteriorates (i.e., when $\Delta T_{pp,LT\,Rec}$ increases), whilst it increases when this performance drop takes place in the HT Rec. These two effects cancel each other out when the ΔT_{pp} of the two recuperators vary simultaneously: in this case, the optimum split flow factor remains virtually constant.

4.3. Comparison with other dopants

Previous sections have shown the good performance of the transcritical *Recompression* cycle applied to CSP plants (i.e., to the corresponding boundary conditions). According to the results presented, thermal efficiencies of ~45% at 550 °C and >51% at 700 °C seem possible when working with 30% SO_2 content. This potential, corresponding to the more conservative assumption of ΔT_{gap}, is now compared against other dopants that were considered in previous publications of the same authors, within the SCARABEUS project, and also against pure CO_2. Fig. 6 shows the thermal efficiency, specific work and temperature rise across the primary heat exchanger of the three cycle configurations considered in earlier sections for each working fluid. Solid bars refer to 550 °C whilst striped bars correspond to 700 °C. The composition of the working mixture is case-sensitive: 85%CO_2–15%C_6F_6 and 83%CO_2–17%$TiCl_4$ for both *Recuperated Rankine* or *Precompression* layouts and 90%CO_2–10%C_6F_6 and 85%CO_2–15%$TiCl_4$ for the *Recompression* cycle. Specific work is expressed in volumetric terms ($W_{s,VOL}$) in order to account for the impact of the largely different density of the working fluids on the size of components. Finally, it is to note that the results for CO_2–C_6F_6 are provided for the lower temperature level only, given that these mixtures have experienced thermal degradation at temperatures higher than 625 °C during the experimental activities carried out by the SCARABEUS consortium (see Table 2).

The results in Fig. 6 confirm that the three CO_2 mixtures yield higher performance than pure CO_2. The thermal efficiency gains experienced at 550 °C are in the order of 7.5, 4.5 and 1.8 percentage points when compared to the simple *Recuperated Rankine*, *Precompression* or *Recompression* cycles respectively, and slightly lower if the higher TIT of 700 °C is considered (around 6.7, 4.3 and 1.7). Nevertheless, it is also true that the mixtures exhibit largely different behaviour when combined with different cycle layouts. For instance, CO_2–C_6F_6 performs best in a *Precompression* layout ($\eta_{th} \approx 43.6\%$ at 550 °C), whilst the potential of CO_2–$TiCl_4$ is fully exploited by the *Recuperated Rankine* layout (η_{th} in the order of 45.7% and 51.5% for 550 °C and 700 °C respectively).[4] Both mixtures have rather poor performance when coupled to a *Recompression* cycle, this being the reason why this cycle layout was dismissed in previous works [44]; interestingly, this particular cycle turns out to be the best option for CO_2–SO_2 mixtures. In this and other aspects (for instance, some thermodynamic properties, Section 2), CO_2–SO_2 mixtures and pure CO_2 behave very similarly (Fig. 6(a)); the reasons for this are discussed in the next section.

From the results presented in this section, it is concluded that the two most interesting cycle options for the SCARABEUS concept are the *Recuperated Rankine* cycle working on CO_2–$TiCl_4$ and the *Recompression* cycle working on CO_2–SO_2, closely followed by the *Precompression* layout with CO_2–C_6F_6 but only for the lower turbine inlet temperature. This ranked list is based on thermal efficiency only and, when $W_{s,VOL}$ and ΔT_{PHE} are also included in the comparison, the benefits attained by CO_2–SO_2 mixtures become larger. At 550 °C, the proposed *Recompression* cycle enables both $W_{s,VOL}$ and ΔT_{PHE} significantly higher than those obtained by $TiCl_4$ (15% and 28.4% respectively), with an expected positive impact on the size and cost of the components of both power block and Thermal Energy Storage system; and the difference becomes even larger at higher TIT. A *Recompression* cycle with CO_2–SO_2 presents 13.7% lower $W_{s,VOL}$ than C_6F_6, but this is compensated for by the higher η_{th} (1 percentage point) and the almost 30% higher ΔT_{PHE}; in both cases, a *Recompression* cycle running on CO_2–SO_2 seems to ensure the best compromise between the three figures of merit. Finally, the superb performance of CO_2–SO_2 mixtures in a *Precompression* cycles is worth noting. This configuration attains $W_{s,VOL}$ and ΔT_{PHE} that are 35% and 50% higher than what can be achieved by CO_2–$TiCl_4$ mixtures, regardless of cycle layout, and over 11% and 46% higher than when using CO_2–C_6F_6.

5. Applicability of transcritical *Recompression* cycles running on CO_2 mixtures

The previous section has shown that the performance of the transcritical *Recompression* cycle depends strongly on the nature of the dopant considered, yielding thermal efficiencies that range from 25% to 45% at 550 °C turbine inlet temperature and from 35% to 51% at 700 °C. In order to investigate this further and to assess the actual applicability of this cycle, the thermal efficiencies for different molar fractions of C_6F_6, $TiCl_4$ and SO_2 are compared in Fig. 7, along with

[4] As a matter of fact, the *Precompression* cycle enables slightly higher η_{th} than the simple recuperated cycle for this mixture but the gain is so limited that the use of a more complex layout is not justified [18].

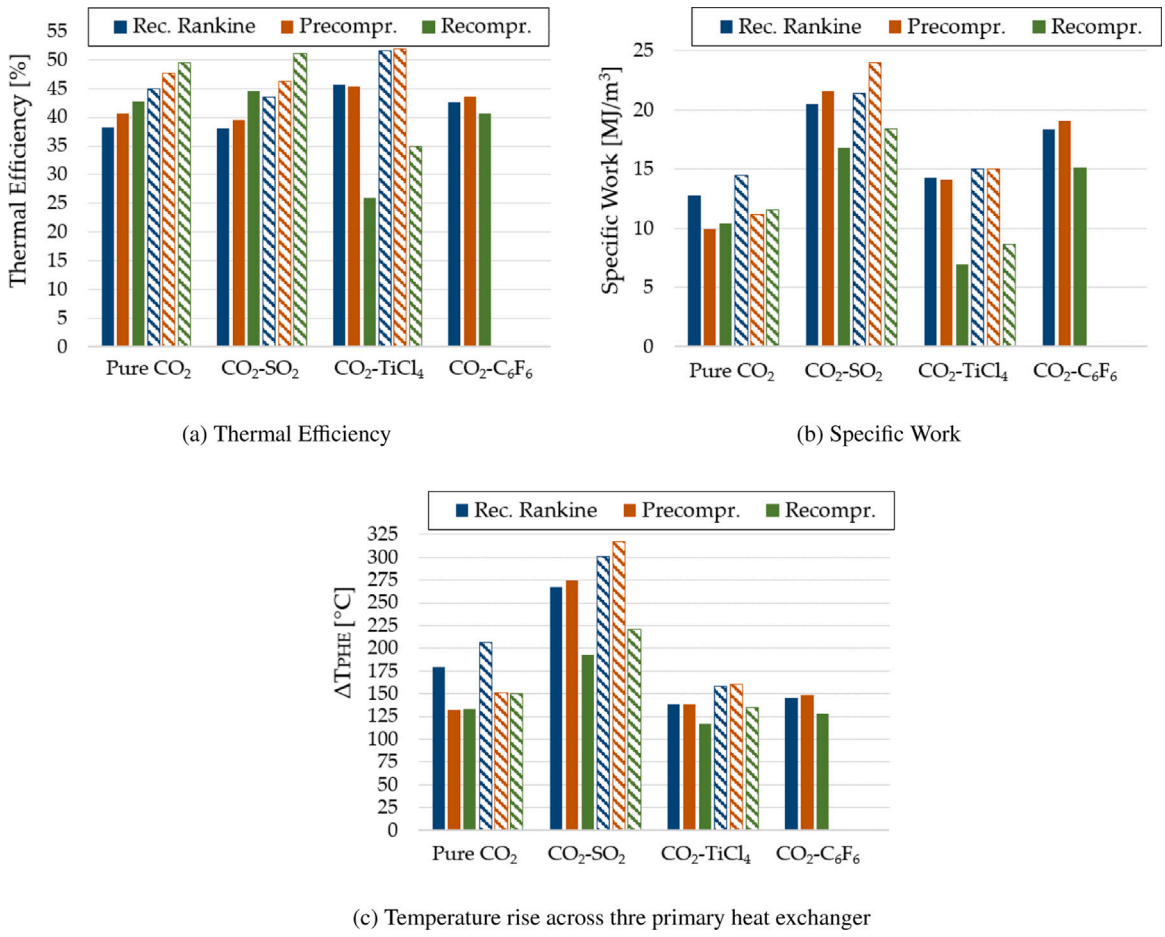

Fig. 6. Performance comparison for different working mixtures, cycle layouts and turbine inlet temperatures. Solid and stripped bars refer to 550 °C and 700 °C respectively. Results for CO_2–C_6F_6 are not reported at 700 °C, due to thermal stability issues.

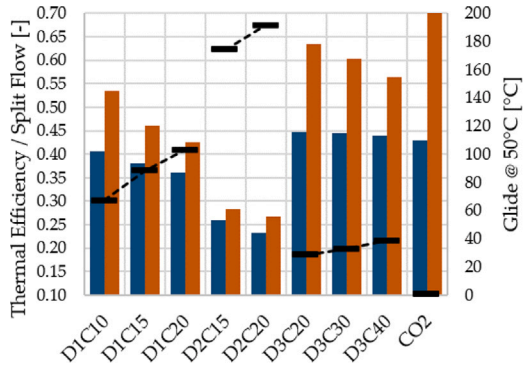

Fig. 7. Thermal efficiency (blue bar), temperature glide (black marker) and split flow factor (brown bar) of a transcritical *Recompression* cycle operating on different CO_2 mixtures. Turbine inlet temperature is set to 550 °C.

the temperature glide of the mixtures considered and the corresponding split flow factors (α). In this section, the analysis is limited to the lower temperature in order to enable the comparison for the entire set of dopants (C_6F_6 is thermally stable up to 625 °C only, see Table 2).

Fig. 7 reveals that higher thermal efficiencies are attained by working mixtures with a smaller temperature glide, as this yields a narrower two-phase region in Fig. 1 providing the recompressor with more flexibility to fully exploit the features of the *Recompression* cycle. For those mixtures with larger glides (C_6F_6 and $TiCl_4$), the recuperator outlet (low-pressure side) falls inside the two-phase region, what is certainly positive in *Recuperated Rankine* cycles because it leads to a lower condenser duty and a higher potential for heat recovery [18,44]. Unfortunately, this is also problematic in terms of the actual practicability of the *Recompression* layout because, in order to successfully operate this cycle, the inlet to the recompressor (station 9 in Fig. 2) must be in superheated state and this implies much lower split flow factors (0.4–0.55 for C_6F_6, <0.3 for $TiCl_4$). These low values of α are detrimental for thermal efficiency as they imply an inevitable performance drop of the low-temperature recuperator. As opposed to this, the narrow two-phase region of CO_2–SO_2 mixtures (small temperature glide) enables having superheated steam at the inlet to the recompressor with suitable split flow factors and this is very beneficial for the cycle from a thermodynamic standpoint, in particular for heat recovery in the low-temperature recuperator, and it leads to significantly higher thermal efficiencies.

For CO_2–SO_2 mixtures, the optimum split flow factor is 0.60, very close to the cycle using pure Carbon Dioxide with the same boundary conditions: 0.71 [18]. This confirms the similar thermodynamic behaviour of CO_2–SO_2 and pure CO_2, which can also be observed in the heat and mass balance provided in Tables 5 and 6 where the corresponding densities and compressibility factors are also fairly similar. The only exceptions to this are stations 1 and 2, pump inlet and outlet sections, whose significantly lower Z in the CO_2–SO_2 case is brought about by fluid condensation. This is the main reason for the enhanced performance of CO_2–SO_2 mixtures as compared to pure CO_2, and confirms the validity of the SCARABEUS concept.

The results presented in this section confirm that the adoption of CO_2–SO_2 mixtures in a *Recompression* cycle is interesting for several reasons. First and foremost, it enables thermal efficiencies that are 2

Table 5
Heat and mass balance of the *Recompression* cycle with pure CO_2. Compressor and turbine inlet temperatures are 50 °C and 700 °C. Maximum cycle pressure is 250 bar. Station numbers as per Fig. 2 (note that the cycle is fully supercritical).

Cycle station	T [°C]	P [bar]	**h** [kJ/kg]	**s** [kJ/kgK]	$\dot{m}$ [kg/s]	ρ [kg/m^3]	Z [–]
1	50.00	102.0	−128.3	−1.18	751	408.6	0.409
2	102.7	250.0	−95.47	−1.17	751	576.1	0.611
3	193.4	246.3	68.37	−0.77	751	330.3	0.846
4	193.7	246.3	68.69	−0.77	1061	330.0	0.846
5	549.2	242.7	525.4	−0.04	1061	149.7	1.044
6	700.0	239.1	716.1	0.18	1061	123.3	1.054
7	585.8	105.1	580.2	0.19	1061	63.67	1.017
8	198.7	104.1	123.5	−0.51	1061	128.0	0.912
9	107.7	103.0	7.52	−0.79	1061	186.5	0.768
10	194.2	246.3	69.46	−0.77	310	329.3	0.847

Table 6
Heat and mass balance of the *Recompression* cycle with 70%CO_2–30%SO_2 (D3C30). Pump and turbine inlet temperatures are set to 50 °C and 700 °C. Maximum cycle pressure is 250 bar. Station numbers as per Fig. 2.

Cycle station	T [°C]	P [bar]	**h** [kJ/kg]	**s** [kJ/kgK]	$\dot{m}$ [kg/s]	ρ [kg/m^3]	Z [–]
1	50.00	68.53	−7520.6	−1.118	464.1	840.1	0.152
2	74.54	250.0	−7497.4	−1.110	464.1	927.1	0.467
3	206.4	246.3	−7247.2	−0.493	464.1	392.8	0.787
4	206.5	246.3	−7246.9	−0.493	769.7	392.6	0.787
5	478.2	242.6	−6909.7	0.072	769.7	190.2	1.021
6	700.0	238.9	−6655.7	0.371	769.7	140.4	1.052
7	534.2	69.93	−6827.1	0.387	769.7	51.87	1.005
8	211.5	69.23	−7164.4	−0.144	769.7	94.96	0.905
9	83.77	68.53	−7315.3	−0.508	769.7	180.1	0.642
10	206.7	246.3	−7246.6	−0.492	305.6	392.2	0.787

percentage points higher than the efficiency attained by pure CO_2 for the same cycle layout and boundary conditions. Second, the similar thermodynamic behaviour of the working fluid enables capitalising the knowledge and technology developed for pure supercritical CO_2 cycles in recent years (thereby avoiding large deviations from the current research and development pathway of the industry and scientific community). In fact, given that even the cycle layout that yields best performance is very likely the same (*Recompression*), it is foreseen that adopting the same part-load and off-design operating strategies as in a sCO_2 cycle would be possible. Of course, this must be confirmed by specific analysis in later stages of this research.

5.1. Influence of minimum cycle temperature

In this last section, the influence of minimum cycle temperature on the optimum molar fraction of Sulphur Dioxide is investigated, with the aim to confirm the results obtained in previous sections and to assess the potential of CO_2–SO_2 cycles at high ambient temperatures. To this end, Fig. 8 illustrates a sensitivity analysis of cycle performance to minimum cycle temperature, when this parameter is varied between 30 °C and 60 °C; results apply to a *Recompression* cycle running on different CO_2/SO_2 mixtures at 700 °C. Solid lines and black markers in the plot refer to cases for which the minimum temperature glide condition is met ($\Delta T_{gap} \geq 30$ °C), whilst dotted lines and white markers refer to cases where $\Delta T_{gap} < 30$ °C. It is worth noting that the mixture with 10% SO_2 content ($y = 0.1$ in Fig. 8) does never comply with this condition $\Delta T_{gap} \geq 30$ °C whereas the mixture with 20% SO_2 satisfies this condition for minimum cycle temperatures lower than 35 °C only. Finally, a dashed line with triangular markers provides the performance of a reference *Recompression* cycle running on pure CO_2 [18].

Fig. 8 confirms that the proposed utilisation of CO_2 mixtures is of interest at high ambient temperatures only. At low minimum cycle temperatures, close to the critical temperature of Carbon Dioxide, the performance of a *Recompression* cycle operating on pure CO_2 ($y = 0$) is similar or even higher than when mixtures are used. On the contrary, at 40 °C (equivalent to ambient temperatures of around 25–30 °C), adding 30% SO_2 yields a 1 percentage point increase in thermal efficiency with respect to the reference case using pure CO_2. If the minimum cycle temperature increases to 45 °C, which is a very likely situation

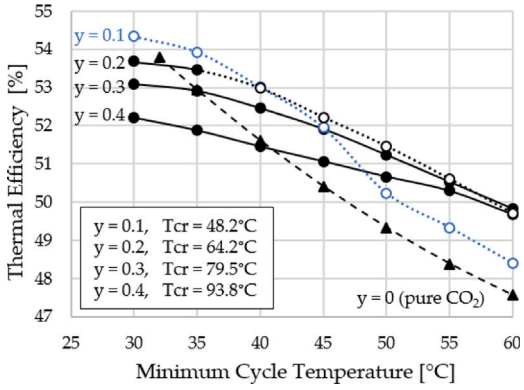

Fig. 8. Sensitivity analysis of cycle performance to minimum cycle temperature. Results are shown for CO_2–SO_2 mixtures with molar fractions of SO_2 between 10% and 40%.

in warm environments, the thermal efficiency difference between pure CO_2 cycles and a cycle with 30% CO_2 content is 1.5 percentage points. Finally, at 60 °C, corresponding to extreme ambient temperatures and air-cooled cycles, the thermal efficiency gain is as high as 2 percentage points.

Another very interesting conclusion from Fig. 8 is that, regardless of ambient temperature, the optimum mixture results to be the one with the minimum Sulphur Dioxide content still complying with the constraint set on the temperature difference between the critical temperature and the temperature at pump inlet (ΔT_{gap}). Furthermore, the impact of SO_2 content on performance is larger at low ambient temperature and decreases at higher temperatures, as seen from the distance between lines of constant y in the plot. This information will be combined with other techno-economic, operational and socio-environmental benefits associated to a lower or higher content of Sulphur Dioxide in the future.

Overall, this last set of results confirms not only the conceptual interest of the SCARABEUS concept but, also, its flexibility and tailorability. Indeed, the plot in Fig. 8 suggests that it is possible to produce a mixture whose composition is optimised for a given set of

Table A.7
Comparison of main cycle figures of merit obtained with Peng–Robinson and PC-Saft Equations of state.

		TIT = 550 °C			TIT = 700 °C		
		D3C20	D3C30	D3C40	D3C20	D3C30	D3C40
Peng Robinson	η_{th} [%]	44.93	44.71	44.10	51.50	51.30	50.82
	W_s [kJ/kg]	94.19	100.3	103.2	122.3	130.3	135.3
	$W_{s,VOL}$ [MJ/m^3]	15.17	16.91	18.20	16.46	18.30	19.82
	ΔT_{PHE} [°C]	176.6	193.6	206.2	200.9	221.9	239.2
PC-SAFT	η_{th} [%]	44.95	44.48	43.45	51.50	51.14	50.40
	W_s [kJ/kg]	93.87	98.66	99.38	121.9	128.7	131.4
	$W_{s,VOL}$ [MJ/m^3]	15.14	16.68	17.58	16.35	18.03	19.22
	ΔT_{PHE} [°C]	178.11	194.0	204.5	201.6	221.6	236.7

Table A.8
Comparison of main cycle figures of merit obtained with PR and PC-Saft Eos: relative deviations Δ.

		TIT = 550 °C			TIT = 700 °C		
		D3C20	D3C30	D3C40	D3C20	D3C30	D3C40
PR vs PC-SAFT	$\Delta(\eta_{th})$ [%]	0.04	0.51	1.47	0.00	0.31	0.83
	$\Delta(W_s)$ [%]	0.34	1.64	3.70	0.37	1.27	2.85
	$\Delta(W_{s,VOL})$ [%]	0.19	1.42	3.43	0.66	1.48	2.99
	$\Delta(\Delta T_{PHE})$ [%]	0.86	0.21	0.82	0.35	0.15	1.03

boundary and operating conditions, not only for a particular plant site but also to account for seasonal variations at a given location. This latter adaptability would however require the ability to control the composition of the mixture in real-time in order to always attain the maximum efficiency for the time-specific ambient temperature; the technical feasibility of this is uncertain since reducing the SO_2 content of the mixture is not a trivial procedure to be performed daily. Another caveats to this would be the impact of the variable composition of the working fluid on the performance of major components like turbomachines and heat exchangers.

6. Conclusions

This paper has analysed the utilisation of mixtures composed of Carbon and Sulphur Dioxides in transcritical *Recompression* cycles, in order to assess the potential of this technology in Concentrated Solar Power plants operating at high ambient temperature. This solution has been compared against similar cycles using pure CO_2 or mixtures of Carbon Dioxide with either Hexafluorobenzene (C_6F_6) or Titaniun Tetrachloride ($TiCl_4$), as already proposed by the authors in past works. Two different turbine inlet temperatures have been considered: 550 °C, representative of state-of-the-art Concentrated Solar Power plants with central receiver, and 700 °C, representative of next generation CSP technology. For the sake of comparison, two other cycle layouts have also been considered: *Recuperated Rankine* and *Precompression*.

The following conclusions are drawn from this work:

- The *Recompression* cycle is the most efficient cycle option to exploit the thermodynamic potential of CO_2–SO_2 mixtures, attaining thermal efficiencies that are 18% and 11% higher than when these mixtures are used in *Recuperated Rankine* and *Precompression* cycles respectively. This is brought about by the particular pressure-temperature envelopes presented by CO_2–SO_2, which are significantly narrower than those of C_6F_6 and $TiCl_4$.
- The *Recompression* cycle enables thermal efficiencies higher than 51% at minimum cycle temperature as high as 50 °C running on CO_2–SO_2, hence stepping forward as a promising alternative for next-generation CSP plants. Furthermore, this mixture enables thermal efficiencies higher than 50% even with minimum cycle temperatures as high as 60 °C.
- From a thermodynamic standpoint, Sulphur Dioxide presents several beneficial features with respect to C_6F_6 and $TiCl_4$, with a globally better compromise between the three main figures of merit considered: thermal efficiency, specific work and temperature rise across primary heat exchanger. Moreover, SO_2 presents high thermal stability and it is not flammable.
- The superior performance of the *Recompression* cycle running on CO_2–SO_2 with respect to the same cycle using pure CO_2 is evident at high minimum cycle temperatures, enabling gains in the order of 2 percentage points, 37% and 30% for η_{th}, W_s and ΔT_{PHE} respectively. The benefits at low turbine inlet temperatures are marginal.
- The molar content of Sulphur Dioxide has a very weak effect on cycle performance when ambient temperatures are high, as long as condensation of the working fluid is enabled ($y \geq 0.2$), whilst the influence becomes stronger at lower temperatures.
- Overall, the *Recompression* cycle operated with 20%–30%(v) SO_2 content yields the most balanced performance for the boundary conditions that are typical of CSP facilities. However, the identification of the optimum mixture composition depends on a thorough multi-objective optimisation based on thermo-economic and LCA analyses. The authors are currently working on this as part of the SCARABEUS project.

Declaration of competing interest

The authors declare that they have no known competing financial interests or personal relationships that could have appeared to influence the work reported in this paper.

Acknowledgements

The SCARABEUS project has received funding from the European Union's Horizon 2020 research and innovation programme under grant agreement Nº 814985. The University of Seville is also gratefully acknowledged for supporting this research through its Internal Research Programme (Plan Propio de Investigación), under contract No 2019/00000359. Last but not least, the regional government of Andalusia (Junta de Andalucía) is gratefully acknowledged for sponsoring the contract of Pablo Rodríguez de Arriba under the Programme for Youth Employment 2014–2020 (Phase 4).

Appendix. Influence of different EoS on cycle performance

This section investigates the influence of using different Equations of state in the estimation of cycle thermal performance. Peng–Robinson and PC-Saft equations of state has been taken into account in this

comparison. These two EoS have been found to be the ones providing the best fit with experimental data found in literature and produced by SCARABEUS consortium experimental activity, led by University of Brescia and Politecnico di Milano. Unfortunately, the complete set of results is still confidential, and it is going to be disclosed soon in another publication developed by these institutions.

In order to consider a wider scenario, thus providing a more reliable comparison, three different Sulphur Dioxide molar fractions have been taken into account — 20%, 30% and 40% — at two different turbine inlet temperature (550 °C and 700 °C). All the results refer to a *Recompression* cycle, and correspond to a minimum cycle temperature of 50 °C.

Table A.7 provides the values obtained for the four main figures of merit taken into account: thermal efficiency (η_{th}), specific work — both mass-flow based (W_s) and volumetric flow-based ($Ws_{s,VOL}$) — and temperature rise across primary heat exchanger (ΔT_{PHE}). Table A.8 presents the relative deviation of these values, obtained comparing the results calculated with the two different equations of state. It results clear that both methodologies achieve very similar results, with relative deviations ranging 0.04–1.5%, 0.34–3.7%, 0.19–3.43% and 0.21–1.03% for η_{th}, W_s, $Ws_{s,VOL}$ and ΔT_{PHE} respectively. Furthermore, it is worth noting that the highest relative deviations refer to D3C40, the mixture achieving the worst thermal performance and thus disregarded in the second part of the present paper. Considering Sulphur Dioxide molar fractions ranging 20%–30%, which are the most interesting according to the conclusions of the present paper, maximum relative deviations results to be lower than 0.51%, 1.7%, 1.5% and 0.86% for η_{th}, W_s, $Ws_{s,VOL}$ and ΔT_{PHE} respectively. Therefore, the conclusion is that the influence of EoS on the estimation of cycle performance is minimum and, as a consequence, Peng–Robinson is a suitable EoS for the scope of the present paper.

References

[1] F. Crespi, G. Gavagnin, D. Sánchez, G.S. Martínez, Supercritical carbon dioxide cycles for power generation: A review, Appl. Energy 195 (2017) 152–183, http://dx.doi.org/10.1016/j.apenergy.2017.02.048.

[2] T. Neises, C. Turchi, Supercritical carbon dioxide power cycle design and configuration optimization to minimize levelized cost of energy of molten salt power towers operating at 650 °C, Sol. Energy 181 (2019) 27–36, http://dx.doi.org/10.1016/j.solener.2019.01.078.

[3] A. Ameli, A. Afzalifar, T. Turunen-Saaresti, J. Backman, Centrifugal compressor design for near-critical point applications, J. Eng. Gas Turbines Power 141 (3) (2019) http://dx.doi.org/10.1115/1.4040691.

[4] J. Lee, J.I. Lee, H.J. Yoon, J.E. Cha, Supercritical carbon dioxide turbomachinery design for water-cooled small modular reactor application, Nucl. Eng. Des. 270 (2014) 76–89, http://dx.doi.org/10.1016/j.nucengdes.2013.12.039.

[5] M.T. White, G. Bianchi, L. Chai, S.A. Tassou, A.I. Sayma, Review of supercritical CO_2 technologies and systems for power generation, Appl. Therm. Eng. 185 (2021) 116447, http://dx.doi.org/10.1016/j.applthermaleng.2020.116447.

[6] A. Romei, P. Gaetani, A. Giostri, G. Persico, The role of turbomachinery performance in the optimization of supercritical carbon dioxide power systems, J. Turbomach. 142 (7) (2020) 071001, http://dx.doi.org/10.1115/1.4046182.

[7] T. Neises, Steady-state off-design modeling of the supercritical carbon dioxide recompression cycle for concentrating solar power applications with two-tank sensible-heat storage, Sol. Energy 212 (2020) 19–33, http://dx.doi.org/10.1016/j.solener.2020.10.041.

[8] D. Alfani, M. Astolfi, M. Binotti, P. Silva, E. Macchi, Off-design performance of CSP plant based on supercritical CO_2 cycles, in: AIP Conference Proceedings, vol. 2303, AIP Publishing LLC, 2020, 130001, http://dx.doi.org/10.1063/5.0029801.

[9] M.D. Carlson, B.M. Middleton, C.K. Ho, Techno-economic comparison of solar-driven sCO_2 brayton cycles using component cost models baselined with vendor data and estimates, in: Energy Sustainability, vol. 57595, American Society of Mechanical Engineers, 2017, http://dx.doi.org/10.1115/ES2017-3590, p. V001T05A009.

[10] N.T. Weiland, B.W. Lance, S.R. Pidaparti, SCO_2 power cycle component cost correlations from DOE data spanning multiple scales and applications, in: Turbo Expo: Power for Land, Sea, and Air, vol. 58721, American Society of Mechanical Engineers, 2019, http://dx.doi.org/10.1115/GT2019-90493, p. V009T38A008.

[11] F. Crespi, D. Sánchez, T. Sánchez, G.S. Martínez, Capital cost assessment of concentrated solar power plants based on supercritical carbon dioxide power cycles, J. Eng. Gas Turbines Power 141 (7) (2019) http://dx.doi.org/10.1115/1.4042304.

[12] C.M. Invernizzi, T. van der Stelt, Supercritical and real gas brayton cycles operating with mixtures of carbon dioxide and hydrocarbons, Proc. Inst. Mech. Eng. A 226 (5) (2012) 682–693, http://dx.doi.org/10.1177/0957650912444689.

[13] M.E. Siddiqui, Thermodynamic performance improvement of recompression brayton cycle utilizing CO_2-C_7H_8 binary mixture, Mechanics 27 (3) (2021) 259–264, http://dx.doi.org/10.5755/j02.mech.28126.

[14] S. Baik, J.I. Lee, Preliminary study of supercritical CO_2 mixed with gases for power cycle in warm environments, in: Turbo Expo: Power for Land, Sea, and Air, vol. 51180, American Society of Mechanical Engineers, 2018, http://dx.doi.org/10.1115/GT2018-76386, p. V009T38A017.

[15] G. Manzolini, M. Binotti, D. Bonalumi, C. Invernizzi, P. Iora, CO_2 mixtures as innovative working fluid in power cycles applied to solar plants. Techno-economic assessment, Sol. Energy 181 (2019) 530–544, http://dx.doi.org/10.1016/j.solener.2019.01.015.

[16] Supercritical CARbon dioxide/alternative fluids blends for efficiency upgrade of solar power plants, 2019, URL https://cordis.europa.eu/project/rcn/221766/factsheet/en. (Accessed 12 May 2021).

[17] M. Binotti, G. Di Marcoberardino, P. Iora, C. Invernizzi, G. Manzolini, SCARABEUS: Supercritical carbon dioxide/alternative fluid blends for efficiency upgrade of solar power plants, in: AIP Conference Proceedings, vol. 2303, AIP Publishing LLC, 2020, 130002, http://dx.doi.org/10.1063/5.0028799.

[18] F. Crespi, P. Rodríguez de Arriba, D. Sánchez, A. Ayub, G. Di Marcoberardino, C.M. Invernizzi, G.S. Martínez, P. Iora, D. Di Bona, M. Binotti, G. Manzolini, Thermal efficiency gains enabled by using CO_2 mixtures in supercritical power cycles, Energy (2021) 121899, http://dx.doi.org/10.1016/j.energy.2021.121899.

[19] D. Bonalumi, S. Lasala, E. Macchi, CO_2-$TiCl_4$ working fluid for high-temperature heat source power cycles and solar application, Renew. Energy 147 (2020) 2842–2854, http://dx.doi.org/10.1016/j.renene.2018.10.018.

[20] G. Di Marcoberardino, E. Morosini, G. Manzolini, Preliminary investigation of the influence of equations of state on the performance of CO_2+C_6F_6 as innovative working fluid in transcritical cycles, Energy (2021) 121815, http://dx.doi.org/10.1016/j.energy.2021.121815.

[21] P. Tafur-Escanta, R. Valencia-Chapi, I. López-Paniagua, L. Coco-Enríquez, J. Muñoz Antón, Supercritical CO_2 binary mixtures for recompression brayton sCO_2 power cycles coupled to solar thermal energy plants, Energies 14 (13) (2021) http://dx.doi.org/10.3390/en14134050.

[22] L. Wang, L.M. Pan, J. Wang, D. Chen, Y. Huang, W. Sun, L. Hu, Investigation on the effect of mixtures physical properties on cycle efficiency in the CO_2-based binary mixtures brayton cycle, Prog. Nucl. Energy (2021) 104049, http://dx.doi.org/10.1016/j.pnucene.2021.104049.

[23] S. Rath, E. Mickoleit, U. Gampe, C. Breitkopf, A. Jäger, Study of the influence of additives to CO_2 on the performance parameters of a sCO_2-cycle, in: Proceedings of 4th European SCO_2 Conference for Energy Systems, sCO2-Flex Project, 2021, http://dx.doi.org/10.17185/duepublico/73965.

[24] O.A. Aqel, M.T. White, M.A. Khader, A.I. Sayma, Sensitivity of transcritical cycle and turbine design to dopant fraction in CO_2-based working fluids, Appl. Therm. Eng. 190 (2021) 116796, http://dx.doi.org/10.1016/j.applthermaleng.2021.116796.

[25] Evaluations of the joint FAO/WHO expert committee on food additives (JECFA), 1998, URL https://apps.who.int/food-additives-contaminants-jecfa-database/chemical.aspx?chemID=985. (Accessed 31 December 2021).

[26] B.D. Horbaniuc, Refrigeration and air-conditioning, in: C.J. Cleveland (Ed.), Encyclopedia of Energy, Elsevier, New York, 2004, pp. 261–289, http://dx.doi.org/10.1016/B0-12-176480-X/00085-1.

[27] PubChem, Compound summary: Sulfur dioxide, 2021, URL https://pubchem.ncbi.nlm.nih.gov/compound/Sulfur-dioxide. (Accessed 31 December 2021).

[28] D.F. Kirk-Othmer, Encyclopedia of Chemical Technology, vol. 23, fourth ed., Wiley Interscience Publication, 2001, http://dx.doi.org/10.1002/0471238961.

[29] NFPA 704: Standard system for the identification of the hazards of materials for emergency response, 2021, URL https://www.nfpa.org/codes-and-standards/all-codes-and-standards/list-of-codes-and-standards/detail?code=704. (Accessed 12 May 2021).

[30] A. S. of Heating, Refrigerating, A.-C. Engineers, ASHRAE Handbook: refrigeration Systems and Applications, American Society of Heating, Refrigerating and Air Conditioning Engineers, 1986.

[31] L. Hanson, L. Ritter, Toxicity and safety evaluation of pesticides, in: R. Krieger (Ed.), Hayes' Handbook of Pesticide Toxicology, third ed., Academic Press, New York, 2010, pp. 333–336, http://dx.doi.org/10.1016/C2009-1-03818-0.

[32] C.M. Invernizzi, Closed power cycles, Lect. Notes Energy 11 (2013) http://dx.doi.org/10.1007/978-1-4471-5140-1.

[33] P. Bombarda, C.M. Invernizzi, Binary liquid metal–organic Rankine cycle for small power distributed high efficiency systems, Proc. Inst. Mech. Eng. A 229 (2) (2015) 192–209, http://dx.doi.org/10.1177/0957650914562094.

[34] N.G. Vannerberg, T. Sydberger, Reaction between SO_2 and wet metal surfaces, Corros. Sci. 10 (1) (1970) 43–49.

[35] Y. Zeng, K. Li, Influence of SO_2 on the corrosion and stress corrosion cracking susceptibility of supercritical CO_2 transportation pipelines, Corros. Sci. 165 (2020) 108404, http://dx.doi.org/10.1016/j.corsci.2019.108404.

[36] NET power's clean energy demonstration plant, La Porte, Texas, 2016, URL https://www.power-technology.com/projects/net-powers-clean-energy-demonstration-plant-la-porte-texas/. (Accessed 12 May 2021).

[37] G. Cui, Z. Yang, J. Liu, Z. Li, A comprehensive review of metal corrosion in a supercritical CO2 environment, Int. J. Greenh. Gas Control 90 (2019) 102814, http://dx.doi.org/10.1016/j.ijggc.2019.102814.

[38] K. Li, Y. Zeng, J.L. Luo, Corrosion of SS310 and alloy 740 in high temperature supercritical CO_2 with impurities H_2O and O_2, Corros. Sci. 184 (2021) 109350, http://dx.doi.org/10.1016/j.corsci.2021.109350.

[39] G. Obulan Subramanian, S.H. Kim, J. Chen, C. Jang, Supercritical-CO_2 corrosion behavior of alumina- and chromia-forming heat resistant alloys with Ti, Corros. Sci. 188 (2021) 109531, http://dx.doi.org/10.1016/j.corsci.2021.109531.

[40] C. Coquelet, A. Valtz, P. Arpentinier, Thermodynamic study of binary and ternary systems containing CO_2+ impurities in the context of CO_2 transportation, Fluid Phase Equilib. 382 (2014) 205–211, http://dx.doi.org/10.1016/j.fluid.2014.08.031.

[41] Thermoflow Inc, Thermoflow suite - Thermoflex software, 2021, URL https://www.thermoflow.com/products_generalpurpose.html. (Accessed 12 May 2021).

[42] Aspen Plus - Leading process simulator software, 2011, URL https://www.aspentech.com/en/products/engineering/aspen-properties. (Accessed 12 May 2021).

[43] G. Angelino, Real gas effects in carbon dioxide cycles 79832, American Society of Mechanical Engineers, 1969, http://dx.doi.org/10.1115/69-GT-102.

[44] F. Crespi, G.S. Martínez, P. Rodríguez de Arriba, D. Sánchez, F. Jiménez-Espadafor, Influence of working fluid composition on the optimum characteristics of blended supercritical carbon dioxide cycles, in: Proceedings of ASME Turbo Expo, American Society of Mechanical Engineers, 2021, http://dx.doi.org/10.1115/GT2021-60293.